PROCEEDINGS OF SPIE

SPIEDigitalLibrary.org/conference-proceedings-of-spie

Determination of the spectral behaviour of atmospheric soot using different particle models

Krzysztof Skorupski

SPIE.

Determination of the spectral behaviour of atmospheric soot using different particle models

Krzysztof Skorupski

Wroclaw University of Science and Technology, Chair of Electronics and Photonics Metrology, Boleslawa Prusa 53/55, 50-317 Wroclaw, Poland

ABSTRACT

In the atmosphere, black carbon aggregates interact with both organic and inorganic matter. In many studies they are modeled using different, less complex, geometries. However, some common simplification might lead to many inaccuracies in the following light scattering simulations. The goal of this study was to compare the spectral behavior of different, commonly used soot particle models. For light scattering simulations, in the visible spectrum, the ADDA algorithm was used. The results prove that the relative extinction error δC_{ext}, in some cases, can be unexpectedly large. Therefore, before starting excessive simulations, it is important to know what error might occur.

Keywords: Light scattering, Black carbon, Soot, Fractal-like aggregates, Discrete Dipole Approximation

1. INTRODUCTION

Small particles connect to each other and create geometries, namely aggregates, which can be described using the following fractal equation:[1,2]

$$N_p = k_f \left(\frac{R_g}{r_p} \right)^{D_f}. \tag{1}$$

in which D_f and k_f are the fractal dimension and the fractal prefactor respectively. N_p is the number of monodisperse primary particles, r_p is their radius and R_g is the radius of gyration, which can be calculated using the formula*:

$$R_g^2 = \frac{1}{N_p} \sum_{i=1}^{N_p} (\bar{r_i} - r_0)^2 = \frac{1}{2N_p^2} \sum_{i,j} (\bar{r_i} - \bar{r_j})^2, \tag{2}$$

where $\bar{r_i}$ is the vector defining the location of the $i-$th primary particle and r_0 is the mass center of the investigated geometry:

$$r_0 = \frac{1}{M} \sum_{i=1}^{N_p} \bar{r_i} m_i. \tag{3}$$

In this equation, M is the total mass of the aggregate and m_i stands for the mass of the $i-$th primary particle. It is a reliable approximation for large, monodisperse aggregates (however, Eq. (1) might be also used when polydispersity is relatively low).

In this paper, soot particles were investigated. Commonly, they can be found in the troposphere.[7] Their core element, namely the fractal-like aggregate of black carbon particles, is a product of incomplete combustion of carbon-based fuels.[8] After generation, it interacts with both organic and inorganic matter and undergo morphological changes in the atmosphere.[9] Here, to create soot particles three materials were used and their complex refractive indices m are presented in Fig. 1. The first of them, namely for black carbon, was adapted from the paper by Chang et al.[10] It is valid for particles generated in propane-oxygen flame. In their experiment, the equivalence ratio was 1.8 and the height above burner was determined as 10mm. Furthermore, the resulting m_c in good agreement with the strict criterion proposed by Bond et al.[8] Next, the refractive index for sulfate

email: krzysztof.skorupski@pwr.edu.pl

*However, alternative equations can be also found in the literature.[3–6]

Laser Communication and Propagation through the Atmosphere and Oceans VI, edited by Jeremy P. Bos, Alexander M. J. van Eijk, Stephen M. Hammel, Proc. of SPIE Vol. 10408, 104080W · © 2017 SPIE
CCC code: 0277-786X/17/$18 · doi: 10.1117/12.2273192

(inorganic matter) was adapted from the OPAC database (the humidity was assumed to be 0%).[11] Finally, the refractive index for organic acids (organic matter) was taken from the work by Myhre et al.[9] The proportion of these three component is not fixed and changes along with the geographical location as well as the age of the soot particle. In many cases, the fraction of black carbon can be 7% (this value was used in the following part of the study) or even less.[12]

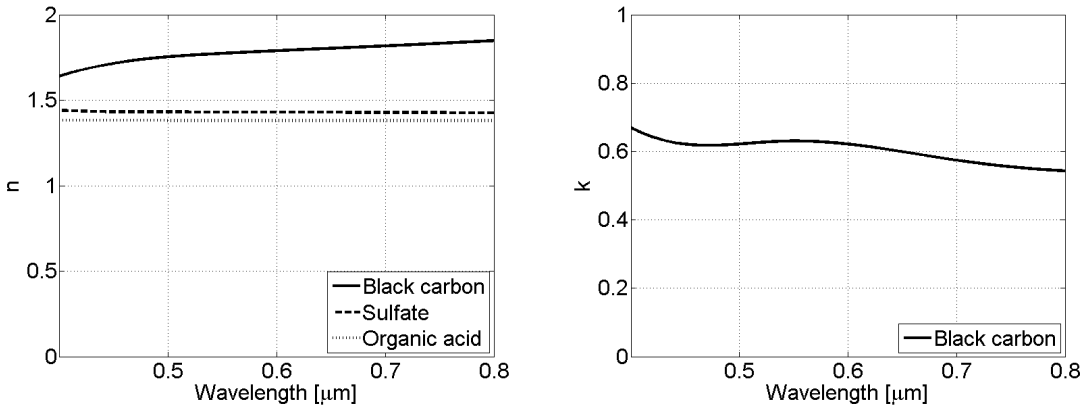

Figure 1. Complex refractive indices m used in the study, namely: black carbon m_c,[10] sulfate m_s,[11] organic acid m_a.[9]

There are many ways and methods to create fractal-like aggregate models. In this work the tunable CC algorithm by Filippov et al.[3] was used. The modification by Skorupski et al.[13] sped up the aggregation process and made the position error almost non-existent[†]. The parameters for creating soot particles were based on various publications.[8,14–21] Note, that many techniques for retrieving morphological parameters are known and each one might lead to slightly different results.[18,19,22–33] Here, the reference black carbon aggregate model was composed of $N_{pc} = 20$ primary particles with the radius $r_p = 15nm$. For the first part of the study, primary particles were spherical and no polydispersity was implemented. To avoid positioning primary particles in point contact, small cylindrical necks, i.e. $Y_a = 0.15$, were added. The neck size parameter is defined as follows:[34,35]

$$Y_a = \frac{r_c}{r_p}, \tag{4}$$

where Y_a is the dimensionless neck size parameter, r_p stands for the radius of the smaller particle and r_c is the radius of the minimum cross section of the investigated neck. The fractal dimension was $D_f = 2.2$ and the fractal prefactor was $k_f = 0.8$. The core fractal-like aggregate model is presented in Fig. 2A.

Light scattering techniques have been commonly used to measure and investigate different objects, like: erythrocytes, fibres, fractal-like aggregates, and much more.[36–42] The absorption properties of black carbon can not be neglected. It is considered as one of the most influential material when the global warming effect is studied.[9,43–47] Here, to measure its optical properties the ADDA algorithm was used. It is based on the DDA (Discrete Dipole Approximation) method which gives accurate results when the investigated geometry is composed of a sufficient number of volume elements (dipoles).[48–52] However, it is less accurate when the material is highly absorbent, like black carbon.[53] For this reason, every primary particle was decomposed into at least $N_d \approx 1000$ volume elements (dipoles). The distance between them in the resulting mesh was $d = 2.4nm$. The polarizability expression was IGT:SO (approximate Integration of Green's Tensor over the dipole). It was proved that it is reliable in the investigated case.[54] Other ADDA parameters were set to their default values. To obtain the most accurate data, all results were orientationally averaged using the Romberg integration technique (the maximum number of orientations was 256).[55,56] A detailed study concerning the use of the DDA method with black carbon particles can be found in the previous work by Skorupski.[54] In the same paper, a comparison between

[†]The algorithm is a part of the FLAGE (Fractal-Like Aggregate Generation Environment) software which can be downloaded from: http://scattering.eu/.

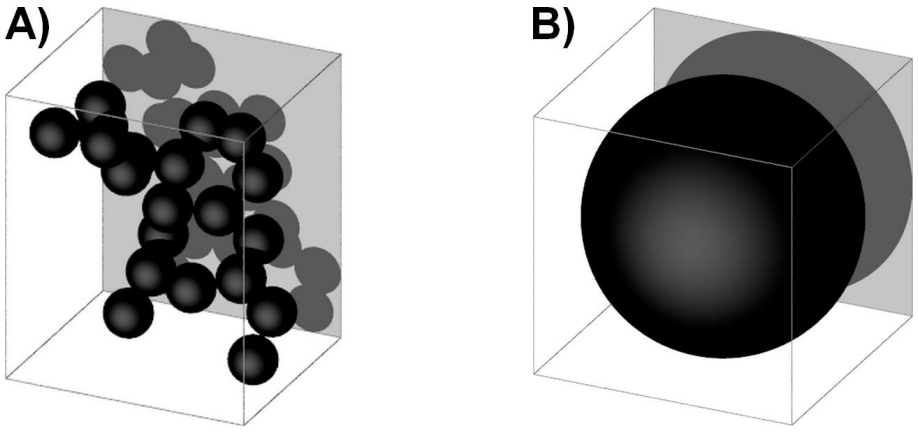

Figure 2. The geometries used for the light scattering simulations: A) The fractal-like aggregate composed of black carbon particles, B) The sphere of equivalent volume.

two scattering methods, namely ADDA and T-Matrix, was performed.[57–60] Here, the incident wavelength varied from $\lambda = 400nm$ to $\lambda = 800nm$ with the step $\Delta\lambda = 50nm$.

2. LIGHT SCATTERING SIMULATIONS

Soot particle models are usually simplified (e.g. to speed up the following light scattering simulations). However, it leads to inaccuracies and simulation errors. In this sections, a few common cases are described.

The most radical simplification is to use, instead of a proper fractal-like aggregate model, a sphere of equivalent volume (Fig. 2B). However, when the extinction cross section C_{ext} is investigated, the changes might not be so extreme, what is presented in Fig. 3. Note, that the results are valid for black carbon aggregates and they prove, that the studied parameter is mostly dependent on the volume.

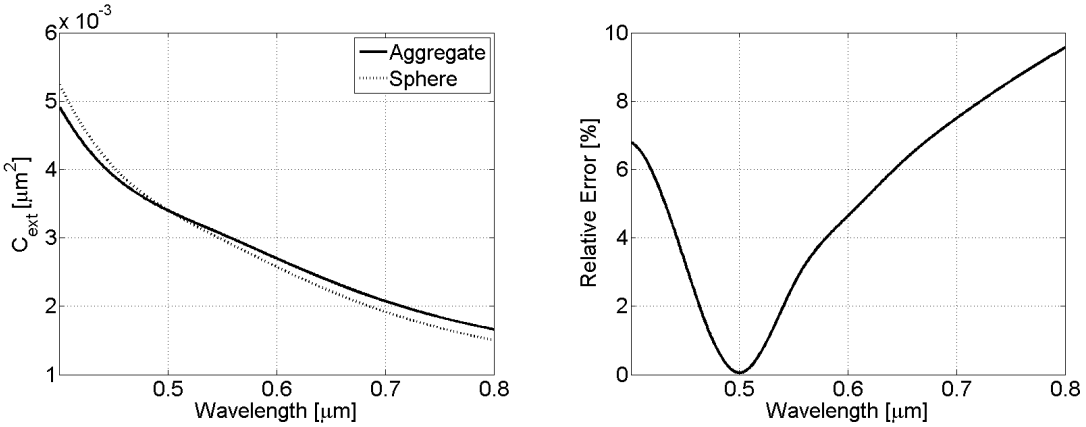

Figure 3. Left) The extinction cross section C_{ext} for the fractal-like aggregate and the sphere of equivalent volume. Right) The relative extinction error δC_{ext} between these models.

Next, five sulfate particles were added to the core geometry (Fig. 4A). Their radius was $r_p = 15nm$. In the next model the five spherical particles were replaced with two ellipsoidal particles (Fig. 4B). However, the sulfate volume remained constant. This is a slightly more realistic approach. The difference in C_{ext} is presented in Fig. 5. It proves that, even when the volume is conserved, the size, shape and location of elements can alter the resulting diagrams. In this case by ca. $\delta C_{ext} \approx 3\%$. Additionally, two more geometries were investigated. The first one was a sphere with an external sulfate layer with the thickness $t_s \approx 3.144nm$ (Fig. 4C). The last

one, used in this part of study, was an equivalent volume sphere, decomposed into a mesh of volume elements (dipoles). There was no strict division between black carbon and sulfate because the location of volume elements (dipoles) was randomized. The total volume of the two materials was always the same. The light scattering simulation results, presented in Fig. 5, were compared to those for the fractal-like aggregate model enriched with two non-spherical particles. Once again, the results prove that the position of elements has an impact on the extinction diagrams and should be taken into consideration before creating realistic soot models.

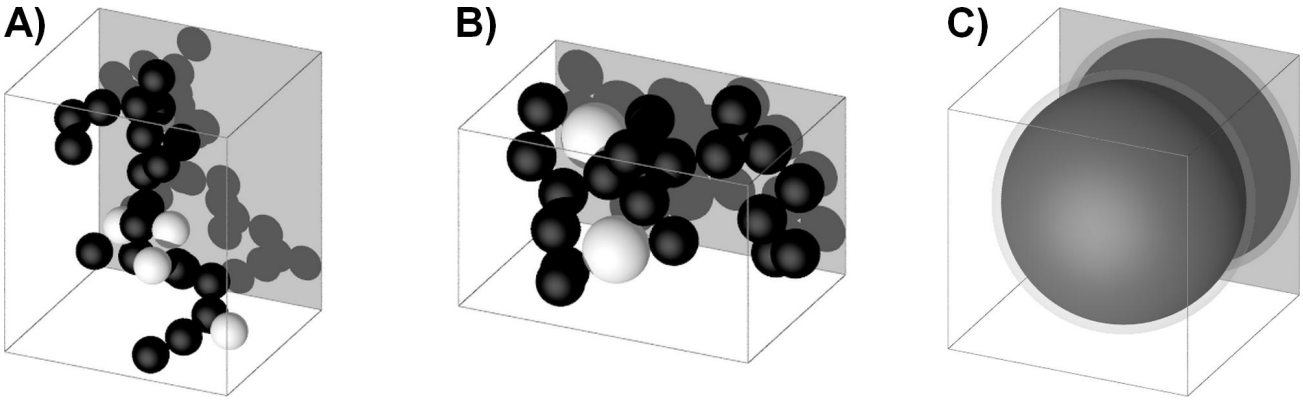

Figure 4. The geometries used for the light scattering simulations: A) The core black carbon aggregate with five spherical sulfate particles. B) The core black carbon aggregate with two ellipsoidal sulfate particles. C) The sphere of equivalent volume.

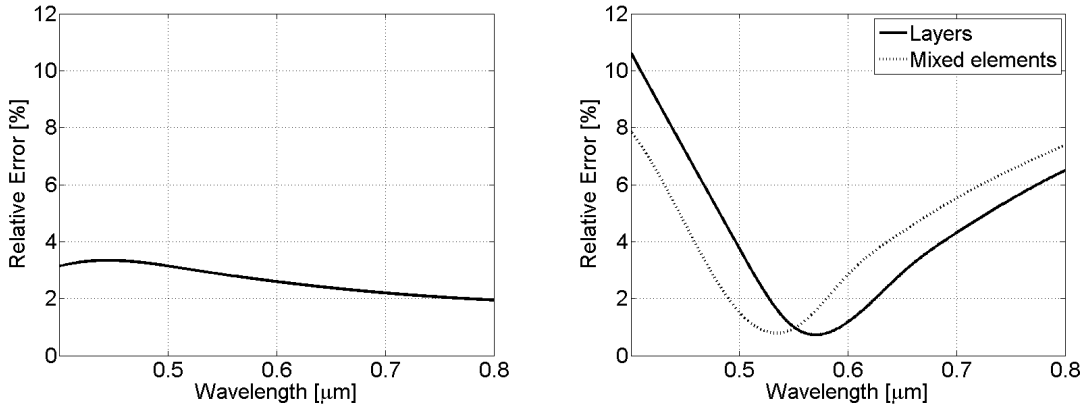

Figure 5. Left) The relative extinction error δC_{ext} between geometries presented in Fig. 4A and Fig. 4B (reference). Right) The relative extinction error δC_{ext} for the two spherical models (covered by the external layers and composed of mixed materials).

In the next study, inorganic matter, i.e. organic acid, was added. Fig. 6A presents the investigated aggregate model composed of $N_{pc} = 15$ black carbon, $N_{ps} = 5$ sulfate, and $N_{pa} = 15$ organic primary particles. All of them were characterized by the radius of $r_p = 15nm$. The light scattering simulations (Fig. 7) were compared to those, obtained by calculating the spectral behavior of a slightly more complex geometry. The more advanced model (Fig. 6B) was composed of $N_{pc} = 15$ spherical black carbon particles, $N_{ps} = 2$ ellipsoidal sulfate particles and an external organic layer with the thickness $t_a = 2.000nm$ (the total volume of the three materials was conserved). This time, by adding organic particles, the geometry was artificially extended what resulted in much more visible discrepancy in C_{ext}. The results prove that external layers should not be modeled as additional particles. Similarly to the previous step, two more spherical geometries were generated. The first one (Fig. 6C) was covered by two layers. The first one was inorganic (sulfate, $t_s \approx 3.144nm$) and the second one was organic

(organic acid, $t_a \approx 5.206$). The second spherical geometry was composed of volume elements (dipoles) in random locations. The results, once again, prove that the extinction cross section C_{ext} is sensitive to the shape and location of materials.

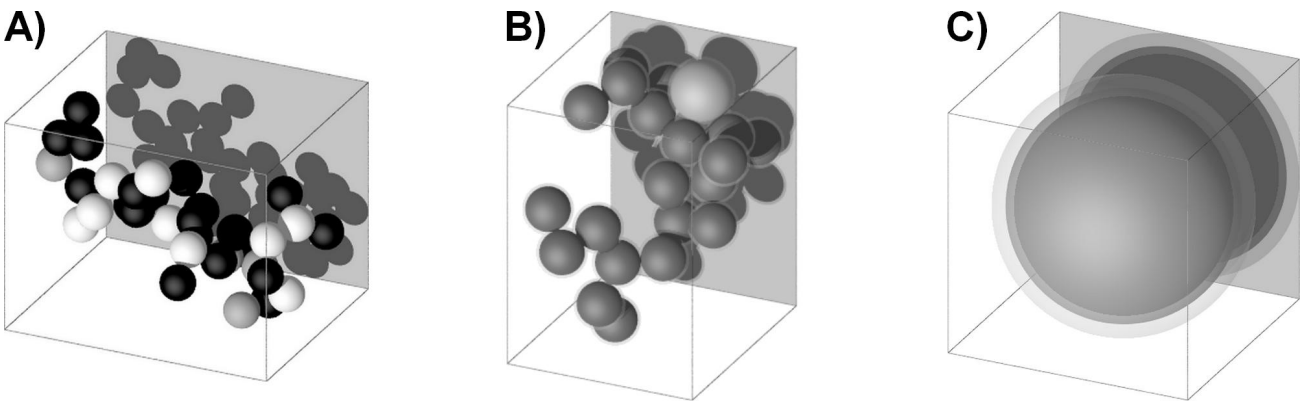

Figure 6. The geometries used for the light scattering simulations: A) The core black carbon aggregate with five spherical sulfate particles and fifteen organic spherical particles. B) The core black carbon aggregate with two ellipsoidal sulfate particles and the organic layer. C) The sphere of equivalent volume.

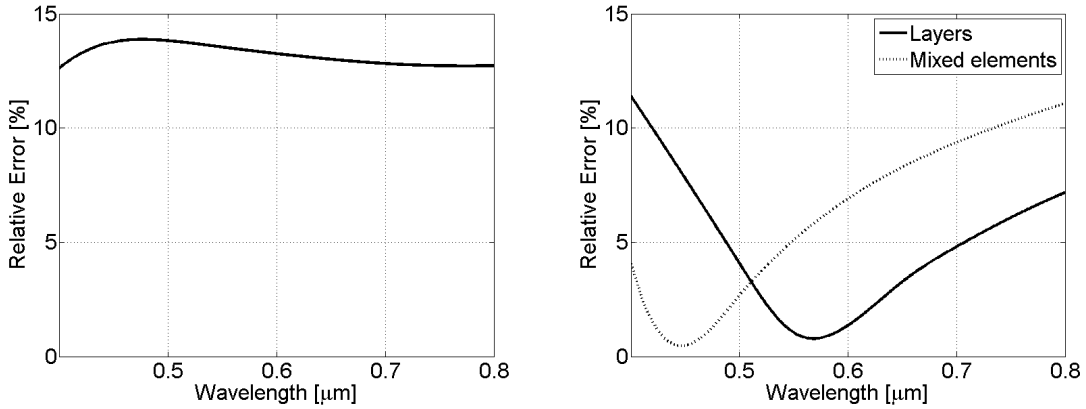

Figure 7. Left) The relative extinction error δC_{ext} between geometries presented in Fig. 6A and Fig. 6B (reference). Right) The relative extinction error δC_{ext} for the two spherical models (covered by the external layers and composed of mixed materials).

Finally, the most advanced soot particle was generated. The normal distribution used for its generation was as follows: the mean particle radius $\bar{r}_{pc} = 15nm$, the standard deviation of the particle radius $\sigma r_{pc} = 1nm$, the mean neck size $Y_a = 0.5$, the standard deviation of the neck size $\sigma Y_a = 0.1$. Again, the fractal dimension was $D_f = 2.2$ and the fractal prefactor was $k_f = 0.8$. Next, two sulfate particles, like in the previous study, were added. All particles were replaced with their equivalent volume ellipsoidal representations. Finally, an external organic layer was added. This time it was much thicker because the volume fraction of black carbon was estimated as 7%. The soot particle model is presented in Fig. 8A. Because the diameter of the resulting geometry was much larger, the distance between volume elements (dipoles) was increased to $d = 3nm$. All the other parameters were the same. The extinction cross section C_{ext} for the whole particle, as well as for its materials, can be found in Fig. 9. As before, two spherical geometries, characterized by the same volume, were generated. The first one, which is the black carbon sphere covered by two additional layers, is presented in Fig. 8B. The second one is an assembly of mixed volume elements (dipoles). This time the results prove that the randomly positioned volume elements (dipoles) lead to much worse results than external, spherical layers.

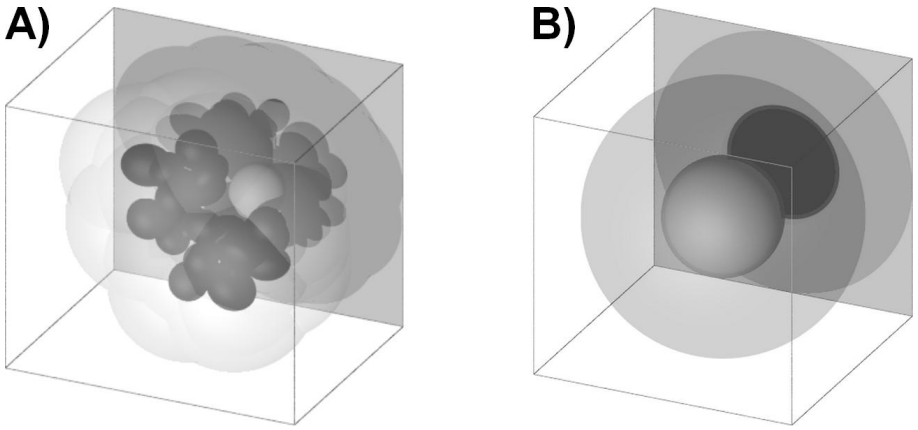

Figure 8. The geometries used for the light scattering simulations: A) The soot particle composed of three materials, namely black carbon, sulfate, organic acid. B) The sphere of equivalent volume.

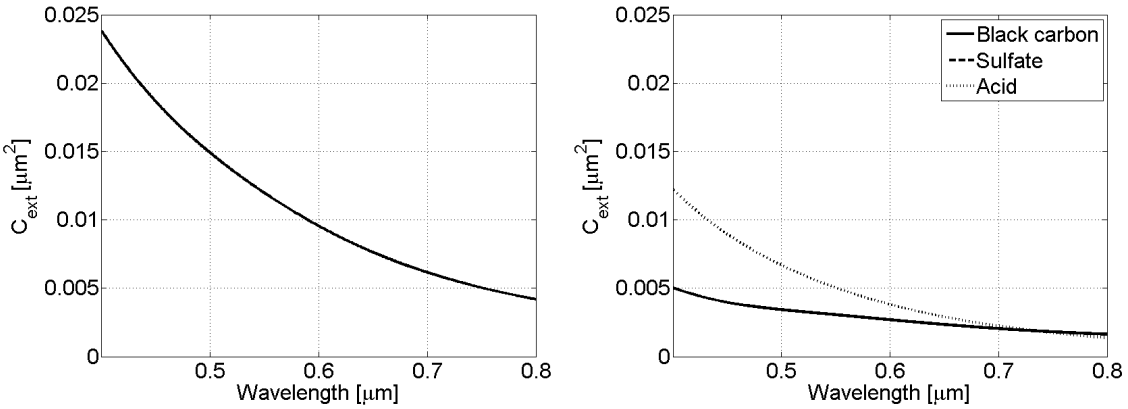

Figure 9. Left) The extinction cross section C_{ext} for the geometry presented in Fig. 6A. Right) The impact of the three materials on the resulting extinction cross section C_{ext}.

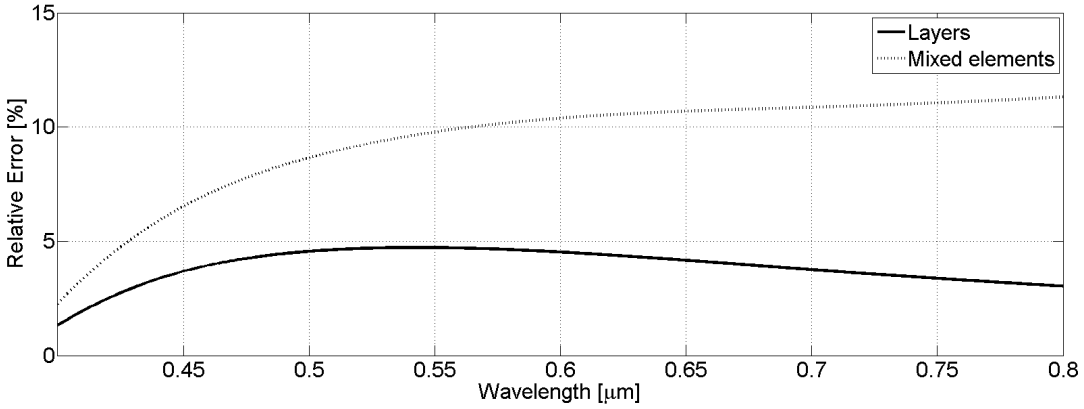

Figure 10. The relative extinction cross section error δC_{ext} for the two spherical models (covered by the external layers and composed of mixed materials). The reference was the geometry presented in Fig. 8A.

3. CONCLUSIONS

In the study three different soot particle models were investigated. The results prove that the position, size and shape of particles has an undeniable impact on the extinction cross section C_{ext}, even when the total volume of used materials remains the same. To improve the quality of simulations of the light scattering process a proper aggregate models must be used.[61]

4. ACKNOWLEDGEMENT

This work is supported by the Polish Ministry of Science and Higher Education, Project No.0402/0121/16

REFERENCES

[1] Sorensen, C. M., "Light scattering by fractal aggregates: A review," *Aerosol Science and Technology* **35**, 648–687 (2001).

[2] Mandelbrot, B., [*The Fractal Geometry of Nature*], W. H. Freeman and Co. (1982).

[3] Filippov, A., Zurita, M., and Rosner, D., "Fractal-like aggregates: Relation between morphology and physical properties," *Journal of Colloid and Interface Science* **229**, 261–273 (2000).

[4] Filippov, A., "Drag and torque on clusters of n arbitrary spheres at low Reynolds number," *Journal of Colloid and Interface Science* **229**, 184–195 (2000).

[5] Oh, C. and Sorensen, C. M., "The effect of overlap between monomers on the determination of fractal cluster morphology," *Journal of Colloid and Interface Science* **193**, 17–25 (1997).

[6] Jackson, G. A., Maffione, R., Costello, D. K., Alldredge, A. L., Logan, B. E., and Dam, H. G., "Particle size spectra between 1 um and 1 cm at Monterey Bay determined using multiple instruments," *Deep Sea Research Part I: Oceanographic Research Papers* **44**, 1739–1767 (1997).

[7] Heintzenberg, J., "Fine particles in the global troposphere: A review," *Tellus* **41B**, 149–160 (1989).

[8] Bond, T. and Bergstrom, R., "Light absorption by carbonaceous particles: An investigative review," *Aerosol Science and Technology* **40**, 27–67 (2006).

[9] Myhre, C. and Nielsen, C., "Optical properties in the UV and visible spectral region of organic acids relevant to tropospheric aerosols," *Atmospheric Chemistry and Physics* **4**, 1759–1769 (2004).

[10] Chang, H. and Charalampopoulos, T., "Determination of the wavelength dependence of refractive indices of flame soot," *Proceedings: Mathematical and Physical Sciences* **430**, 577–591 (1990).

[11] Hess, M., Koepke, P., and Schult, I., "Optical properties of aerosols and clouds: The software package OPAC," *Bulletin of the American Meteorological Society* **79**, 831–844 (1998).

[12] Adachi, K., Chung, S. H., and Buseck, P. R., "Shapes of soot aerosol particles and implications for their effects on climate," *Journal of geophysical research* **115**, D15206 (2010).

[13] Skorupski, K., Mroczka, J., Wriedt, T., and Riefler, N., "A fast and accurate implementation of tunable algorithms used for generation of fractal-like aggregate models," *Physica A: Statistical Mechanics and its Applications* **404**, 106–117 (2014).

[14] Bond, T., "Spectral dependence of visible light absorption by carbonaceous particles emitted from coal combustion," *Geophysical Research Letters* **28**, 4075–4078 (2001).

[15] Adachi, K. and Buseck, P. R., "Internally mixed soot, sulfates, and organic matter in aerosol particles from Mexico City," *Atmospheric Chemistry and Physics* **8**, 6469–6481 (2008).

[16] Adachi, K., Chung, S. H., Friedrich, H., and Buseck, P. R., "Fractal parameters of individual soot particles determined using electron tomography: Implications for optical properties," *Journal of geophysical research* **112, doi:10.1029/2006JD008296** (2007).

[17] Katrinak, K., Rez, P., Perkes, P., and Buseck, P., "Fractal geometry of carbonaceous aggregates from an urban aerosol," *Environmental Science and Technology* **27**, 539–547 (1993).

[18] Oltmann, H., Reimann, J., and Will, S., "Single-shot measurement of soot aggregate sizes by wide-angle light scattering (WALS)," *Applied Physics B: Lasers and Optics* **106**, 171–183 (2012).

[19] Oltmann, H., Reimann, J., and Will, S., "Wide-angle light scattering (WALS) for soot aggregates characterization," *Combustion and Flame* **157**, 516–522 (2010).

[20] Poppel, L. L., Friedrich, H., Spinsby, J., Chung, S. H., Seinfeld, J. H., and Buseck, P. R., "Electron tomography of nanoparticle clusters: Implications for atmospheric lifetimes and radiative forcing of soot," *Geophysical Research Letters* **32,doi:10.1029/2005GL024461** (2005).

[21] Burtscher, H., "Physical characterization of particulate emissions from diesel engines: A review," *Journal of Aerosol Science* **36**, 896–932 (2005).

[22] Mroczka, J. and Szczuczyski, D. K., "Inverse problems formulated in terms of first-kind fredholm integral equations in indirect measurements," *Metrology and Measurement Systems* **16**, 333–357 (2009).

[23] Mroczka, J. and Szczuczyski, D. K., "Improved regularized solution of the inverse problem in turbidimetric measurements," *Applied Optics* **5**, 4591 (2010).

[24] Mroczka, J. and Szczuczyski, D. K., "Problem odwrotny - jako rekonstrukcji funkcji rozkadu wielkoci czstek w pomiarach nefelometrycznych i turbidymetrycznych," *PAK* **9**, 246–249 (2007).

[25] Mroczka, J. and Szczuczyski, D. K., "Simulation research on improved regularized solution of the inverse problem in spectral extinction measurements," *Applied Optics* **51**, 1715–1723 (2012).

[26] Mroczka, J., Wozniak, M., and Onofri, F. R. A., "Algorithms and methods for analysis of the optical structure factor of fractal aggregates," *Metrology and Measurements Systems* **19**, 459–470 (2012).

[27] Will, S., Schraml, S., Bader, K., and A.Leipertz, "Performance characteristics of soot primary particle size measurements by time-resolved laser-induced incandescence," *Applied Optics* **37**, 5647–5658 (1998).

[28] Iuliis, S. D., Cignoli, F., and Zizak, G., "Two-color laser-induced incandescence (2C-LII) technique for absolute soot volume fraction measurements in flames," *Applied Optics* **44**, 7–8 (2005).

[29] Ryser, R., Gerber, T., and Dreier, T., "Soot particle sizing during high-pressure diesel spray combustion via time-resolved laser-induced incandescence," *Combustion and Flame* **156**, 120–129 (2009).

[30] Wozniak, M., Onofri, F. R. A., Barbosa, S., Yon, J., and Mroczka, J., "Comparison of methods to derive morphological parameters of multi-fractal samples of particle aggregates from TEM images," *Journal of Aerosol Sciance* **47**, 12–26 (2012).

[31] Brasil, A., Farias, T., and Carvalho, G., "A recipe for image characterization of fractal-like aggregates," *Journal of Aerosol Science* **30**, 1379–1389 (1999).

[32] Czerwinski, M., Mroczka, J., Girasole, T., Gouesbet, G., and Grehan, G., "Light-transmittance predictions under multiple-light-scattering conditions. i. direct problem: hybrid-method approximation," *Applied Optics* **40**, 1514–1524 (2001).

[33] Czerwinski, M., Mroczka, J., Girasole, T., Gouesbet, G., and Grehan, G., "Light-transmittance predictions under multiple-light-scattering conditions. ii. inverse problem: particle size determination," *Applied Optics* **40**, 1525–1531 (2001).

[34] Skorupski, K., Mroczka, J., Riefler, N., Oltmann, H., Will, S., and Wriedt, T., "Effect of the necking phenomenon on the optical properties of soot particles," *Journal of Quantitative Spectroscopy and Radiative Transfer* **141**, 40–48 (2014).

[35] Skorupski, K., Hellmers, J., Feng, W., Mroczka, J., Wriedt, T., and Mdler, L., "Influence of sintering necks on the spectral behaviour of ITO clusters using the discrete dipole approximation," *Journal of Quantitative Spectroscopy and Radiative Transfer* **159**, 11–18 (2015).

[36] Wriedt, T., Hellmers, J., Eremina, E., and Schuh, R., "Light scattering by single erythrocyte: Comparison of different methods," *Journal of Quantitative Spectroscopy and Radiative Transfer* **100**, 444–456 (2006).

[37] Nilsson, A., Alsholm, P., Karlsson, A., and Andersson-Engels, S., "T-matrix computations of light scattering by red blood cells," *Applied Optics* **37**, 2735–2748 (2000).

[38] Mroczka, J. and Wysoczanski, D., "Plane-wave and gaussian-beam scattering on an infinite cylinder," *Optical Engineering* **39**, 736–770 (2000).

[39] Girasole, T., Gouesbet, G., Grehan, G., Toulouzan, J. L., Mroczka, J., Ren, K., and Wysoczanski, D., "Cylindrical fibre orientation analysis by light scattering. part ii: Experimental aspects," *Particle and Particle Systems Characterization* **14**, 211–218 (1997).

[40] Girasole, T., Bultynck, H., Gouesbet, G., Toulouzan, J. L., Mroczka, J., Ren, K., and Wysoczanski, D., "Cylindrical fibre orientation analysis by light scattering. part i: Numerical aspects," *Particle and Particle Systems Characterization* **14**, 163–174 (1997).

[41] Girasole, T., Toulouzan, J. L., Mroczka, J., and Wysoczanski, D., "Fiber orientation and concentration analysis by light scattering: Experimental setup and diagnosis," *Review of Scientific Instruments* **68**, 2805–2811 (1997).
[42] Skorupski, K., Mroczka, J., Riefler, N., Oltmann, H., Will, S., and Wriedt, T., "Impact of morphological parameters onto simulated light scattering patterns," *Journal of Quantitative Spectroscopy and Radiative Transfer* **119**, 53–66 (2013).
[43] Ebert, M., Weinbruch, S., Rausch, A., Gorzawski, G., Hoffman, P., Wex, H., and Helas, G., "Complex refractive index of aerosols during LACE 98 as derived from the analysis of individual particles," *Journal of Geophysical Research* **107**, D21 (2002).
[44] Kahnert, M. and Devasthale, A., "Black carbon fractal morphology and short-wave radiative impact: A modelling study," *Atmospheric Chemistry and Physics* **11**, 11745–11759 (2011).
[45] Bond, T., Doherty, S., Fahey, D., Forster, P., Berntsen, T., DeAngelo, B., Flanner, M., Ghan, S., Karcher, B., Koch, D., Kinne, S., Kondo, Y., Quinn, P., Sarofim, M., Schultz, M., Schulz, M., Venkataraman, C., Zhang, H., Zhang, S., Bellouin, N., Guttikunda, S., Hopke, P., Jacobson, M., Kaiser, J., Klimont, Z., Lohmann, U., Schwarz, J., Shindell, D., Storelvmo, T., Warren, S., and Zender, C. S., "Bounding the role of black carbon in the climate system: A scientific assessment," *Journal of Geophysical Research: Atmospheres* **118**, 5380–5552 (2013).
[46] Andreae, M. and Gelencser, A., "Black carbon or brown carbon? The nature of light-absorbing carbonaceous aerosols," *Atmospheric Chemistry and Physics* **6**, 3131–3148 (2006).
[47] Jacobson, M., "Climate response of fossil fuel and biofuel soot, accounting for soot's feedback to snow and sea ice albedo and emissivity," *Journal of Geophysical Research: Atmospheres* **109**, D21201 (2004).
[48] Yurkin, M. and Hoekstra, A., "The discrete dipole approximation: An overview and recent developments," *Journal of Quantitative Spectroscopy and Radiative Transfer* **106**, 558–589 (2007).
[49] Yurkin, M. and Hoekstra, A., "The discrete-dipole-approximation code ADDA: Capabilities and known limitations," *Journal of Quantitative Spectroscopy and Radiative Transfer* **112**, 2234–2247 (2011).
[50] Draine, B. T. and Flatau, P. J., "User guide for the discrete dipole approximation code ddscat 7.2," *Instrumentation and Methods for Astrophysics* (2012).
[51] Draine, B. T. and Flatau, P. J., "Discrete dipole approximation for scattering calculations," *Journal of the Optical Society of America A* **11**, 1491–1499 (1994).
[52] Penttila, A., Zubko, E., Lumme, K., Muinonen, K., Yurkin, M., Draine, B., Rahola, J., Hoekstra, A., and Shkuratov, Y., "Comparison between discrete dipole implementations and exact techniques," *Journal of Quantitative Spectroscopy and Radiative Transfer* **106**, 417–436 (2007).
[53] Skorupski, K., "The optical properties of tropospheric soot aggregates determined with the DDA (Discrete Dipole Approximation) method," *Proc. SPIE 9526, Modeling Aspects in Optical Metrology V* (doi:10.1117/12.2184634, 2015).
[54] Skorupski, K., "Using the DDA (discrete dipole approximation) method in determining the extinction cross section of black carbon," *Metrology and Measurement Systems* **22**, 153–164 (2015).
[55] Davis, P. J. and Rabinowitz, P., [*Methods of Numerical Integration*], New York: Academic Press (1975).
[56] Riefler, N., Stasio, S., and Wriedt, T., "Structural analysis of clusters using configurational and orientational averaging in light scattering analysis," *Journal of Quantitative Spectroscopy and Radiative Transfer* **89**, 323–342 (2004).
[57] Waterman, P. C., "Symmetry, unitarity and geometry in electromagnetic scattering," *Physical Review D* **3**, 825–839 (1971).
[58] Mishchenko, M. I., Travis, L. D., and Mackowski, D. W., "T-matrix computations of light scattering by nonspherical particles: a review," *Journal of Quantitative Spectroscopy and Radiative Transfer* **55**, 535–575 (1996).
[59] Mishchenko, M. I. and Travis, L. D., "Capabilities and limitations of a current fortran implementation of the t-matrix method for randomly oriented, rotationally oriented symetric scatters," *Journal of Quantitative Spectroscopy and Radiative Transfer* **60**, 309–324 (1998).
[60] Mackowski, D. and Mischenko, M., "A multiple sphere t-matrix fortran code for use on parallel computer clusters," *Journal of Quantitative Spectroscopy and Radiative Transfer* **112**, 2182–2192 (2011).
[61] Mroczka, J., "The cognitive process in metrology," *Measurements* **46**, 2896–2907 (2013).